Two-Phase Cooling of Targets and Electronics for Particle Physics Experiments

J.R. Thome, J.A. Olivier, J.E. Park
Laboratory of Heat and Mass Transfer (LTCM), École Polytechnique Fédérale de Lausanne (EPFL)
Station 9, CH-1015 Lausanne, Switzerland

john.thome@epfl.ch

Abstract

An overview of the LTCM lab's decade of experience with two-phase cooling research for computer chips and power electronics will be described with its possible beneficial application to high-energy physics experiments. Flow boiling in multi-microchannel cooling elements in silicon (or aluminium) have the potential to provide high cooling rates (up to as high as 350 W/cm^2), stable and uniform temperatures of targets and electronics, and lightweight construction while also minimizing the fluid inventory. An overview of two-phase flow and boiling research in single microchannels and multi-microchannel test elements will be presented together with video images of these flows. The objective is to stimulate discussion on the use of two-phase cooling in these demanding applications, including the possible use of CO_2.

I. INTRODUCTION

Flow boiling in microchannels has become one of the "hottest" research topics in heat transfer. Numerous experimental studies on boiling in microchannels have appeared over the past decade, especially in the past few years. Most tests have been done with refrigerants but tests have also been done with water, acetone, CO_2, etc.

A. Electronics cooling application

As an example of the two phase cooling application, the microelectronics and power electronics industries are now facing the challenge of removing very high heat fluxes of 300 W/cm^2 or more while maintaining their operating temperature below the targeted temperature, such as 85°C for CPUs. Although conventional cooling solutions, such as air-cooled heat sinks, have been used successfully until now, no straightforward extension is expected for such high heat fluxes. Alternative solutions such as jet impingement cooling, single-phase and two-phase cooling in microchannels have been explored and showed different advantages or drawbacks [1]. Figure 1 shows the heat sink thermal resistances for diverse cooling technologies as a function of the pumping power to the dissipated thermal power ratio. The best heat sink solution should be that nearest the lower left axis intersection point because it represents the lowest thermal resistance at the lowest pumping power. Recent literature on two-phase flow boiling in microchannels does not yet show a race to achieve very high heat fluxes compared to single-phase flow or jet cooling studies, although it yields much lower pressure drops and a much higher overall efficiency (dissipated power/pumping power). The fact that the fluid temperature varies very little during the vaporization process and that the heat transfer coefficient increases with heat flux are also major advantages.

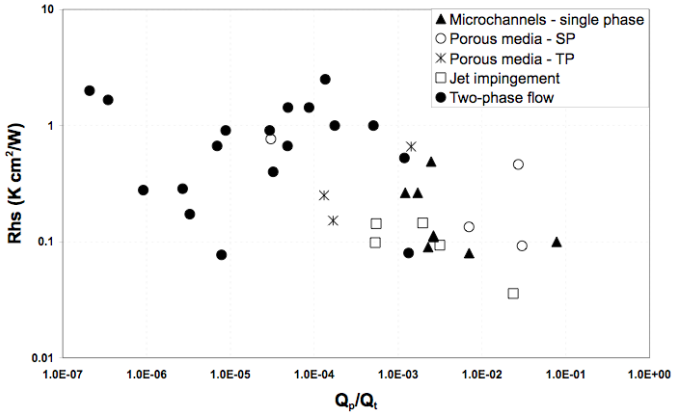

Figure 1: Thermal resistance of heat sinks for diverse cooling technologies as a function of the pump to the dissipated power ratio from Agostini *et al.* [1].

B. Microchannel effect

It is worth noting that what happens in small channels in two-phase flows can be quite different than that for single-phase flows in small channels. While initial studies in the literature reported significant size effects on friction factors and heat transfer coefficients in very small channels in single-phase flows, more accurate recent tests and analysis done with very smooth internal channels have shown that macroscale methods for single-phase flows work well at least down to diameters of 5-10 microns. This is not the case for macroscale two-phase flow methods, which usually do not work very well when compared to data for channels below about 2.0 mm diameter. Thus, it is very risky to extrapolate macroscale two-phase flow pattern maps, flow boiling methods and two-phase pressure drop correlations to the microscale, except for specific documented cases. Furthermore, many of the controlling phenomena and mechanisms change when passing from macroscale two-phase flow and heat transfer to the microscale. For example, surface tension (capillary) forces become much stronger as the channel size diminishes while gravitational forces are weakened. Therefore, it is usually not sensible to empirically refit macroscale methods to microscale data since the underlying physics has substantially changed, which means that different dimensionless groups are now controlling and/or come into play.

Figure 2 depicts the buoyancy effect on an elongated bubble in 2.0, 0.790 and 0.509 mm horizontal channels. In the 2.0 mm channel, no stratified flow was observed while the difference in film thickness at the top compared to that at the bottom is still quite noticeable. Similarly, the film thickness in

the 0.790 mm channel is still not uniform above and below the bubble. Instead, in the 0.509 mm channel, the film is now quite uniform. Interpreting these images and many others available in the literature, one ascertains that in small, horizontal channels that stratified-wavy and fully stratified flows disappear (more or less completely). This transition is thus perhaps an indication of the lower boundary of macroscale two-phase flow, in this case occurring for a diameter somewhat greater than 2.0 mm. The upper boundary of microscale two-phase flow may be interpreted as the point in which the effect of gravity becomes insignificant, such that the bubble in the 0.509 mm channel is thus a microscale flow, with the transition occurring at about this diameter at the present test conditions.

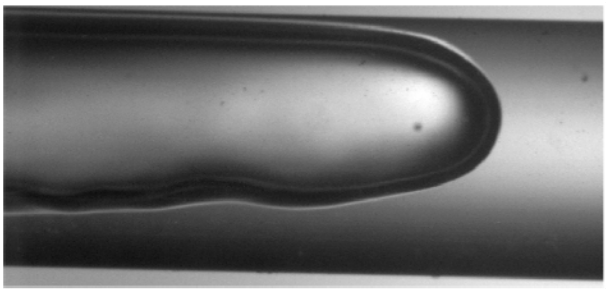

(a) 2.0 mm

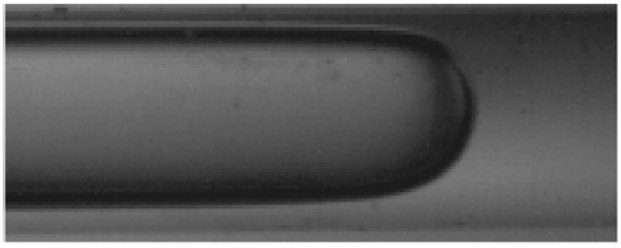

(b) 0.790 mm

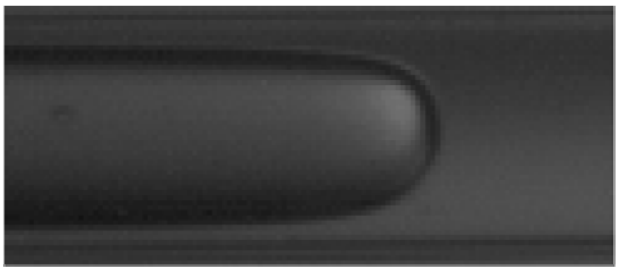

(c) 0.509 mm

Figure 2: Video images of slug (elongated bubble) flow in a 2.0, 0.8 and 0.5 mm horizontal channels with R-134a at 30°C at the exit of a micro-evaporator channel of the same diameter (images by R. Revellin of LTCM).

II. PREDICTION METHODS

Numerous applications for microscale flow boiling are emerging: high heat flux cooling of computer microprocessor chips and power electronics, cooling of micro-reactors, micro-heat pumps and micro-refrigerators, automotive evaporators with multi-port aluminium tubes, etc. All of these applications require thermal design methods that are accurate, reliable and robust (that is, methods that follow the trends of data well and work for a multitude of fluids, microchannel sizes and shapes, pressures, flow rates, applications, etc.). Presently, the state-of-the-art is only partially able to fulfil such requirements.

A. Heat transfer model

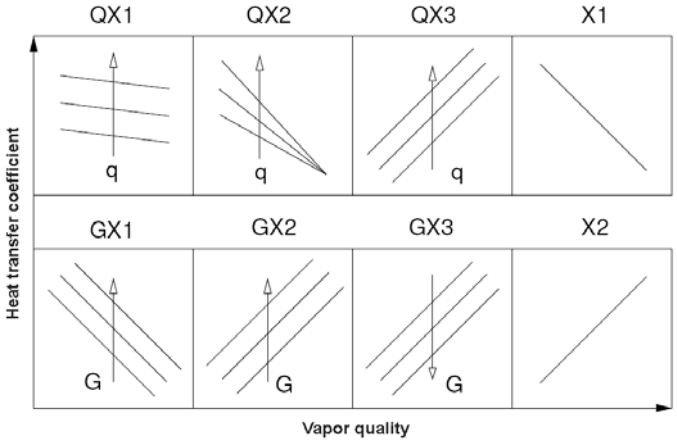

Figure 3: Heat transfer trends versus vapor quality documented by Agostini and Thome [2] from 13 different studies on boiling in microchannels.

Agostini and Thome [2], based on a review of 13 published studies, analyzed the numerous trends in the heat transfer data. Figure 3 shows a composite diagram of these trends in the local flow boiling heat transfer coefficient plotted versus the vapor quality (defined as the rate of the mass flow rate of the vapor to that of the total flow) and denotes whether or not the heat transfer coefficient varied with another parameter or not, where an arrow with the symbol shows the direction of the variation with this parameter. For instance, QX1 means that the heat transfer coefficient decreased with increasing vapor quality but at the same time the heat transfer coefficient increased with increasing heat flux. QX2 showed a similar trend except that the data all came together at a higher vapor quality. In contrast, QX3 describes data in which the heat transfer coefficient increased with vapor quality and with heat flux. The X1 data type decreased sharply with vapor quality but did not depend on mass velocity or heat flux whereas X2 refers to data sets that only increased with vapor quality while were insensitive to mass velocity and heat flux. The GX1, GX2 and GX3 showed three types of trends with respect to mass velocity and vapor quality.

The majority of the studies found boiling heat transfer trends represented by QX1 and X1 (11 out of 13). It was thus concluded generally that:

- at very low vapor qualities ($x < 0.05$), the heat transfer coefficient either tends to increase with vapor quality or is insensitive to vapor quality while it increases with heat flux (not shown);
- at low to medium vapor qualities ($0.05 < x < 0.5$), the heat transfer coefficient increases with heat flux

and decreases or is relatively constant with respect to vapor quality;

- at higher vapor qualities (x > 0.5), the heat transfer coefficient decreases sharply with vapor quality and does not depend on heat flux or mass velocity;
- the effect of heat flux is always to increase the heat transfer coefficient except at high x where it tends to have little effect (more recent studies show however that at very high heat flux its effect diminishes and then may even create a decrease in heat transfer with a further increase in heat flux;
- the influence of mass velocity varies from no effect, an increasing effect or a decreasing effect.

These conflicting trends, which are different than the simple trends typically found in macroscale flow boiling, appear to point to the influence of additional phenomena, channel geometry, surface roughness and heat transfer mechanisms coming into play in microchannel boiling. Thus, heat transfer coefficients are extremely difficult to predict. Most of the existing heat transfer models are empirical correlations.

Jacobi and Thome [3] proposed the first theoretically-based, elongated bubble (slug) flow boiling model for microchannels, modelling the thin film evaporation of the liquid film trapped between these bubbles and the channel wall and also accounting for the liquid-phase convection in the liquid slugs between the bubbles. The focus of their study was to demonstrate that the thin film evaporation mechanism was the principal heat transfer mechanism controlling heat transfer in slug flows in microchannels, not nucleate boiling as cited in many experimental studies where that conclusion was based solely on the basis of heat transfer coefficient vs. heat flux data plotting up like a nucleate pool boiling curve but without actual observations (and by extrapolation of macroscale ideology to the microscale).

Following this initial work, a three-zone flow boiling model for slug (elongated bubble) flow in microchannels was proposed by Thome *et al.* [4], i.e. an updated version of the prior two-zone model of Jacobi and Thome [3]. Figure 4 shows a representation of the three-zone model where L_p is the total length of the pair or triplet, L_L is the length of the liquid slug, L_G is the length of the bubble including the length of the dry wall of the vapor slug L_{dry}, and L_{film} is the length of the liquid film trapped by the bubble. The internal radius and the diameter of the tube are R and d_i while δ_o and δ_{min} are the thicknesses of the liquid film trapped between the elongated bubble and the channel wall at its formation and at dry out of the film (only when dry out occurs). The evolution of successive bubbles is shown in the lower diagram. The local vapor quality, heat flux, microchannel internal diameter, mass flow rate and fluid physical properties at the local saturation pressure are input parameters to the model. The three-zone model predicts the heat transfer coefficient of each zone and the local time-averaged heat transfer coefficient of the cycle at a fixed location along a microchannel during evaporation of an elongated bubble at a constant, uniform heat flux boundary condition. The elongated bubbles are assumed to nucleate and quickly grow to the channel size upstream such that successive elongated bubbles are formed that are confined by the channel and grow in axial length, trapping a thin film of liquid between the bubble and the inner tube wall as they flow along the channel. The thickness of this film plays an important role in heat transfer. At a fixed location, the process is assumed to proceed as follows: (i) a liquid slug passes (without any entrained vapor bubbles, contrary to macroscale flows which often have numerous entrained bubbles), (ii) an elongated bubble passes (whose liquid film is formed from liquid removed from the liquid slug) and (iii) a vapor slug passes if the thin evaporating film of the bubble dries out before the arrival of the next liquid slug. The cycle then repeats itself upon arrival of the next liquid slug at a frequency f ($=1/\tau$). Thus, a liquid slug and an elongated bubble pair or a liquid slug, an elongated bubble and a vapor slug triplet pass this fixed point at a frequency f that is a function of the formation and coalescence rate of the bubbles upstream.

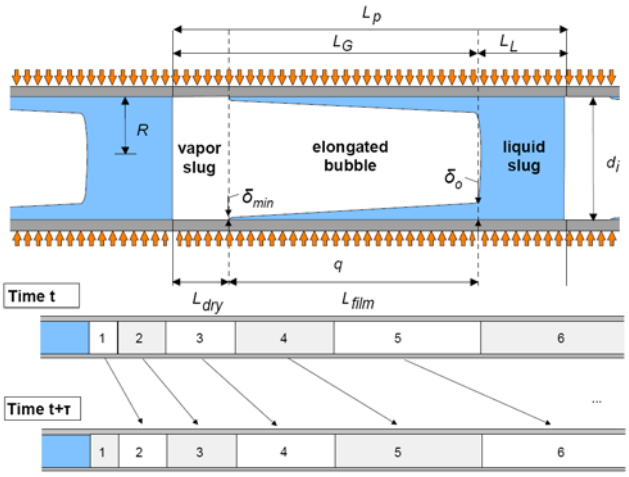

Figure 4: Three-zone heat transfer model of Thome *et al.* [4] for elongated bubble flow regime in microchannels. *Top*: Diagram illustrating a triplet comprised of a liquid slug, an elongated bubble and a vapor slug; *bottom*: Bubble tracking of a *triplet* with passage of a new bubble at time intervals of τ.

B. *Pressure drop model*

The two principle approaches to predict frictional pressure gradients in microscale two-phase flow are the homogeneous and the separated flow models. The homogenous model assumes that the two-phase fluid behaves as a single-phase fluid but uses pseudo-properties for the density and viscosity that are weighted relative to the vapor and liquid flow fractions. It is also assumed that the liquid and vapour flow at the same velocity, which is evidenced in slug flow within microchannels. The separated flow model considers that the phases are artificially segregated into two streams, one liquid and one vapor, and interact through their common interface.

An extensive comparison was done by Ribatski *et al.* [5]. Among them, the homogeneous model, the simplest model, predicted the data better than other, more complicated models, for a wide range of test conditions.

III. COOLANT FLUIDS

CO_2 is a natural refrigerant and has been intensively investigated for automobile air-conditioning, refrigeration and

heat pump systems over the past decade [6-11]. It has no ozone depletion potential (ODP = 0) and a negligible direct global warming potential (GWP = 1).

The physical and transport properties of CO_2 are quite different from those of conventional refrigerants at the same saturation temperatures. CO_2 has higher liquid and vapor thermal conductivities, a lower vapor-liquid density ratio (lower liquid and higher vapor densities), a very low surface tension, and a lower liquid-vapor viscosity ratio (lower liquid and higher vapor viscosities) than conventional refrigerants. Thus, flow boiling heat transfer, two-phase flow pattern and pressure drop characteristics are quite different from those of conventional low pressure refrigerants. Previous experimental studies have shown that CO_2 has higher flow boiling heat transfer coefficients and lower pressure drops than those of common refrigerants at the same saturation temperature [6, 7, 9, 11]. However, it must be realized that the operational pressure of CO_2 is much higher than other conventional refrigerants such as R134a and R245fa. Figure 5 compares the saturation pressure and temperature curves for several radiation-hard fluids. It is seen that the most likely candidate for low-temperature operations would be CO_2 and C_2F_6. These fluids will be investigated in the next section.

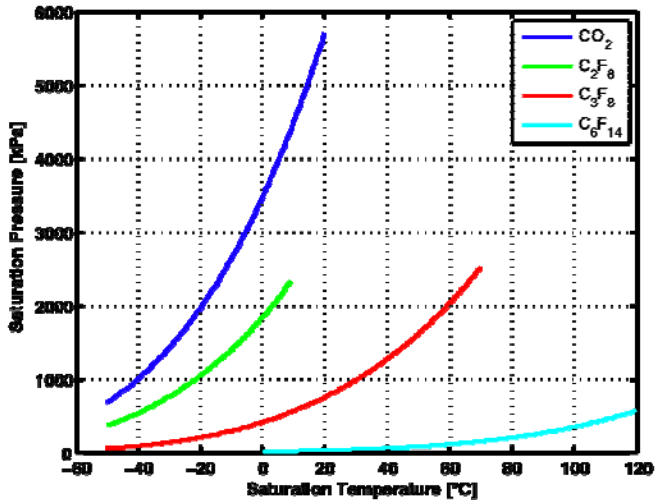

Figure 5: Saturation curves for radiation-hard fluids

IV. Simulation

Simulations will be performed on a rectangular multi-microchannel as shown in the schematic in Figure 6. The simulations will compare single-phase flow to two-phase flow and are aimed at the cooling of a high precision silicon pixel detector, also called the GigaTracKer (GTK), being developed at CERN.

Some specifications regarding the GTK are that the channels should be as small as possible, with fin heights not being greater than 50 µm, although simulations will be run on higher fin heights. The fin width can be made as small as possible, although mechanical integrity must be maintained.

The GTK has a total width of 60 mm with channel lengths being 30 mm. Channel lengths should be as short as possible as to reduce the total inlet-to-outlet temperature difference for single-phase flow and to keep the outlet vapor quality as low as possible for two-phase flow (due to a decrease in heat transfer coefficients for qualities greater than 0.4).

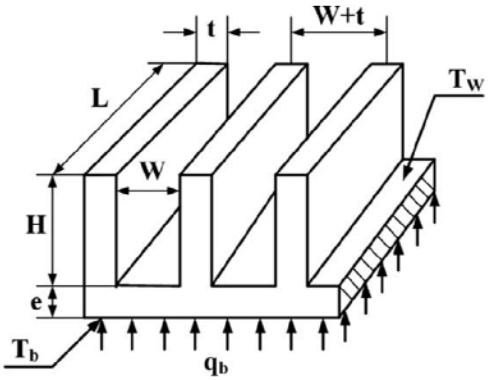

Figure 6: Schematic of a multi-microchannel evaporator

In all cases, the base thickness, *e*, will be zero, thus showing a best-case scenario as any additional material added can be accounted for in separate calculations. It is also stated that the GTK should not see a temperature difference of more than 5˚C while being kept as cold as possible (~ -30˚C).

Assumptions made for the present simulations are: (*1*) the evaporator is uniformly heated from the bottom with a base heat flux of q_b, (*2*) the flow through the cooler is uniformly distributed between all the channels, (*3*) the top of the cooler is adiabatic and (*4*) for two-phase flow, no inlet subcooling is used. The models used for single-phase heat transfer and pressure drop are those from Shah and London [12], while the three-zone model [4] and homogeneous model were used for the two-phase heat transfer and pressure drop, respectively. The homogeneous model was used as it predicts the pressure drops within microchannels with fair accuracy [5].

The fluid to be simulated will be radiation-hard fluor-carbons and CO_2. The saturations curves of these fluids were given in Figure 5. The choice of fluids depends on the desired operating condition. For temperatures below -10˚C, the best choice of fluid would be between CO_2 and C_2F_6 but possibly also C_3F_8. The most common cooling fluid used at CERN is C_6F_{14} and is used in single-phase flows only. This fluid is not ideal for two-phase cooling as it is a low-pressure fluid, having a saturation temperature of 56˚C at atmospheric pressure, implying that the system would need to be under vacuum for lower temperatures. This has the disadvantage that one is limited by the allowable pressure drop within the cooling device, implying that channels should be relatively large. The potential of air also leaking into the system becomes greater, having serious consequences regarding the performance of the cooling device. Thus, for two-phase cooling, CO_2, C_2F_6 and C_3F_8 will be compared.

A. Single-Phase Flow

Figure 7 shows the effects the channel width and height have on the maximum base temperature difference relative to the inlet and the pressure drop. In both cases the channel width was kept constant at 50 µm while varying the fin height, and vice versa. The fin width was kept at 25 µm. A base heat flux of 2 W/cm^2 was applied while maintaining the mass flux at 4500 kg/m^{2}s. From the simulation, it is seen that

the major contribution is in the increase of the fin height. By doubling the fin height the temperature difference and pressure drop are decreased by about 50%. Any further increase does not improve the performance by much. Thus, ideally the channel width should be kept at 50 µm with the fin height at 100 µm. For the given footprint dimensions this translates into 799 parallel channels.

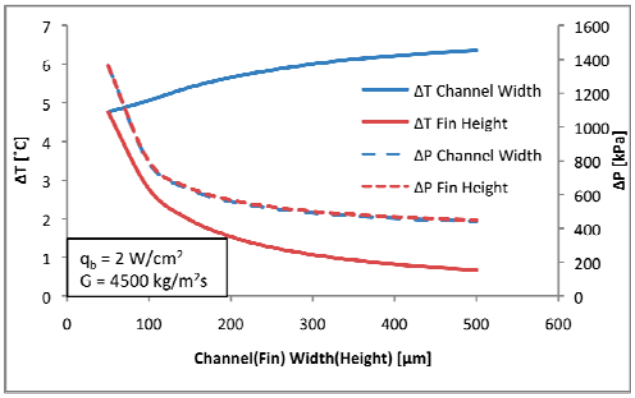

Figure 7: Effect of channel width and fin height on maximum base temperature difference and pressure drop for single-phase flow using C_6F_{14} as the working fluid

B. *Two-Phase Flow*

The three fluids to be used in two-phase simulation are CO_2, C_2F_6 and C_3F_8. Due to the low saturation pressure of C_3F_8, all simulations will be performed at a saturation temperature of -1˚C. The actual local temperatures and pressures for the three refrigerants are shown in Figure 8. The pressures are shown in terms of the ratio of the local pressure to the inlet pressure. As seen, although the process is two-phase, the base temperature is not always constant and is dependent on the fluid. This is due to the dry out of the liquid film of the elongated bubble (*viz.* Figure 4). The film thickness is directly a function of the enthalpy of vaporisation with CO_2 having a value almost 3 times higher than the other refrigerants, thus having a thicker film, which inevitably does not dry out for the current conditions. Pressure drops are also significantly less for CO_2 and C_2F_6 since their viscosities are about half that of C_3F_8.

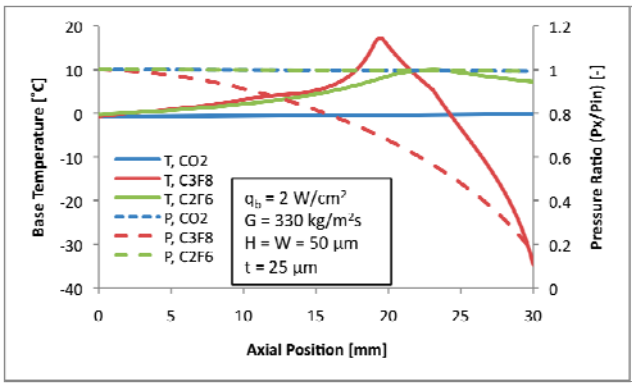

Figure 8: Local temperature and pressure drops for CO_2, C_3F_8 and C_2F_6 during two-phase flow

Figure 9 shows the maximum base temperature difference relative to the inlet and the pressure drop as a function of the fin height. The fin height has a major effect with C_3F_8, decreasing the temperature difference and pressure drop by almost 700% by doubling the height. The temperature difference also becomes less for C_2F_6 with the increase in fin height, with hardly any effect on the pressure drop. These simulations show that the highest pressure fluid, CO_2, is best suited for small geometries as temperature gradients and pressure drops are small.

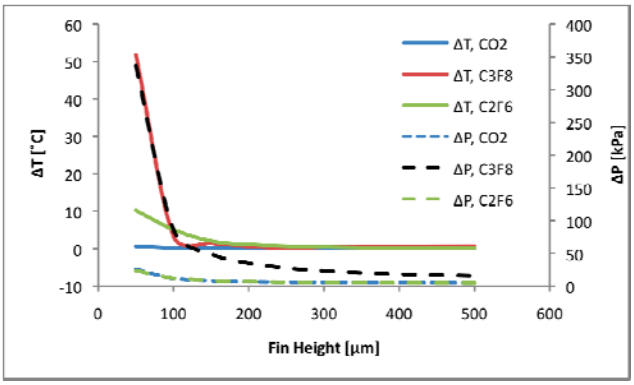

Figure 9: Effect of fin height on maximum base temperature difference and pressure drop for two-phase flow

C. *Single-Phase vs. Two-Phase*

Figure 10 shows a comparison of single-phase to two-phase cooling. The single-phase fluid used was C_6F_{14} with the inlet temperature of -30˚C while the two-phase fluid was CO_2 with an inlet saturation temperature of -30˚C. The fin height and channel width were 50 µm, while the fin thickness was 25 µm. A base heat flux of 2 W/cm^2 was applied. The diagram shows the actual junction/base temperature and fluid pressure versus the axial position along the channel. For both the single-phase and two-phase results the axial temperature difference is below 5˚C, although the increase in temperature for the two-phase fluid is much less than for the single-phase fluid (0.14˚C vs. 4.7˚C). The difference in the fluids' pressure drops is even more significant. The single-phase fluid requires a mass flux of 4500 kg/m^{2}s to obtain a temperature difference of less than 5˚C and has a pressure drop of about 700 kPa! The two-phase fluid only required a mass flux of 250 kg/m^{2}s that resulted in a pressure drop of 60 kPa. The power required to move the two fluids is 1984 mW and 28 mW, respectively. This also implies that any advantage gained from using a single-phase fluid due to overall system pressure is negated due to the high pressure drops, unless changes to the geometry are made.

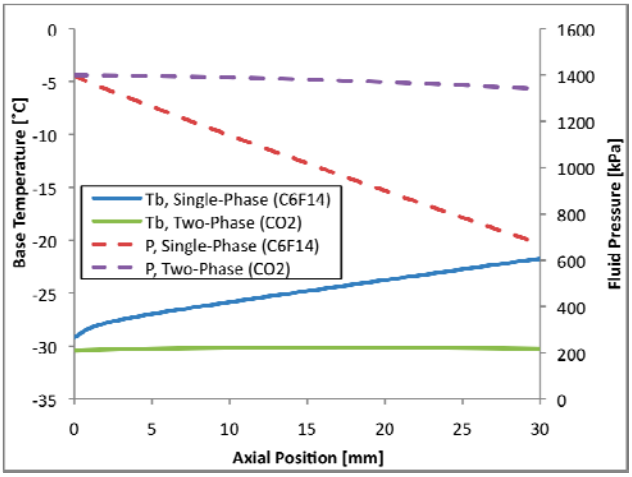

Figure 10: Single-phase vs. two-phase cooling

V. Design Considerations

Several design considerations are needed for safe operation of the cooling system. Although a large international effort is underway on two-phase heat transfer research, the physical mechanisms involved are still not fully understood, particularly instabilities and critical heat flux.

A. Critical heat flux

For high heat flux cooling applications using multi-microchannel cooling channels, the critical heat flux (CHF) in saturated flow boiling conditions is a very important operational limit. It signifies the maximum heat flux that can be dissipated at the particular operating conditions. Surpassing CHF means that the heated wall becomes completely and irrevocably dry, and is associated with a very rapid and sharp increase in the wall temperature due to the replacement of liquid by vapor adjacent to the heat transfer surface. For example, Figure 11 illustrates the onset of CHF in multi-microchannel tests showing the temperature excursion that occurs during small steps of increasing heat flux. For most applications, this temperature excursion will result in irreparable damage to the device being cooled. Thus, critical heat flux is a particularly important design parameter in microchannel boiling applications in determining the upper operating limit of the cooling system for safe, reliable operation.

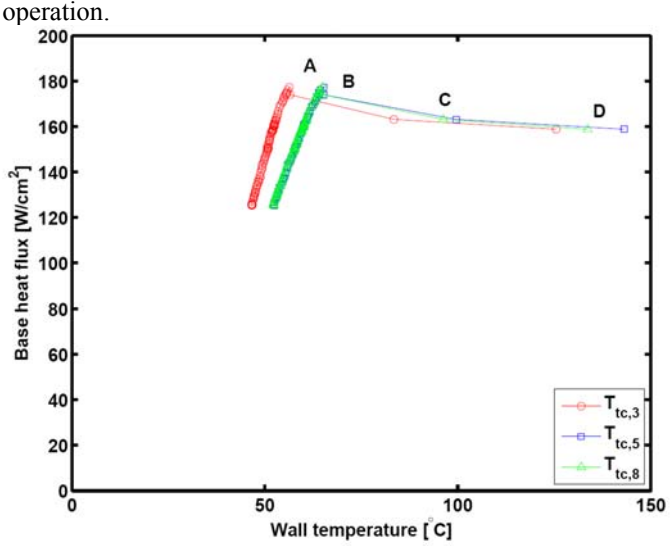

Figure 11: Flow boiling curve measured at three different positions along the channel showing the onset of critical heat flux from Park [13].

Revellin and Thome [14] have proposed a theoretically based model for predicting critical heat flux in microchannels. Their model is based on the premise that CHF is reached when local dryout occurs during evaporation in annular flow at the location where the height of the interfacial waves reaches that of the annular film's mean thickness. To implement the model, they first solve one-dimensionally the conservation of mass, momentum and energy equations assuming annular flow to determine variation of the annular liquid film thickness δ, ignoring any interfacial wave formation, along the channel. Then, based on the slip ratio and a Kelvin-Helmoltz critical wavelength criterion (assuming the film thickness to be proportional to the critical wavelength of the interfacial waves), the wave height was modelled with the following empirical expression:

$$\Delta\delta = 0.15\left(\frac{u_G}{u_L}\right)^{-\frac{3}{7}}\left(\frac{g(\rho_L-\rho_G)(d_i/2)^2}{\sigma}\right)^{-\frac{1}{7}}$$

Then, when δ equals Δδ at the outlet of the microchannel, CHF is reached. Refer to Figure 12 for a simulation. The leading constant and two exponents were determined with a database including three fluids (R-134a, R-245fa and R-113) and three circular channel diameters (0.509 mm, 0.790 mm and 3.15 mm) taken from the CHF data of Wojtan *et al.* [15] and Lazarek and Black [16]. Their model also satisfactorily predicted the R-113 data of Bowers and Mudawar [17] for circular multi-microchannels with diameters of 0.510 and 2.54 mm of 10 mm length. Furthermore, taking the channel width as the characteristic dimension to use as the diameter in their 1-d model, they were also able to predict the rectangular multi-microchannel data of Qu and Mudawar [18] for water. All together, 90% of the database was predicted within ±20%. As noted above, this model also accurately predicted the R-236fa multi-microchannel data of Agostini *et al.* [19]. Furthermore, in a yet to be published comparison, this model also predicts CHF data of CO_2 in microchannels from three additional independent studies.

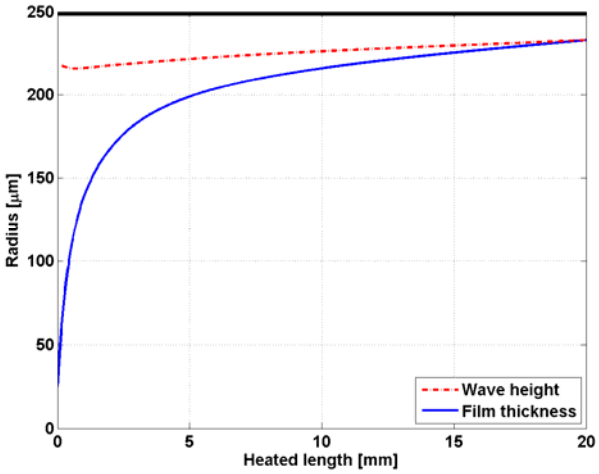

Figure 12: Revellin and Thome [14] CHF model showing the annular film thickness variation along the channel plotted versus the wave height. The simulation is for R-134a at a saturation temperature of 30°C in a 0.5 mm channel of 20 mm heated length without inlet subcooling for a mass velocity of 500 kg/m^{2}s, yielding a CHF of 396 kW/m^2

B. *Flow instabilities*

Multi-microchannel flow boiling test sections can suffer from flow maldistribution and backflow effects, where some channels have a higher liquid flow rate than others. The flow may in fact flow back into the inlet header and some channels may become prematurely dry from too low of an inlet liquid flow rate. Such instabilities and maldistribution must be avoided completely to have a safe, reliable design.

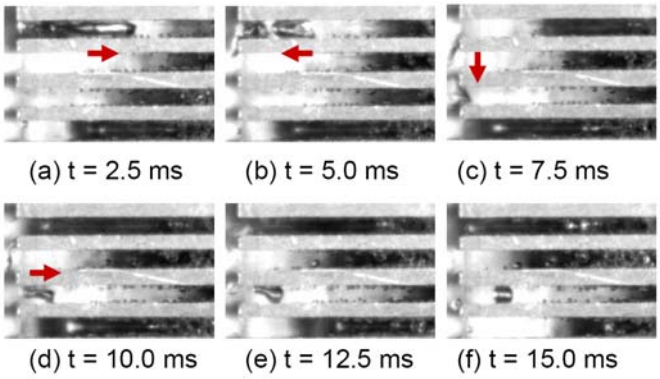

Figure 13: Dramatic effect that maldistribution can have on the heat transfer process from Park et al. [20].

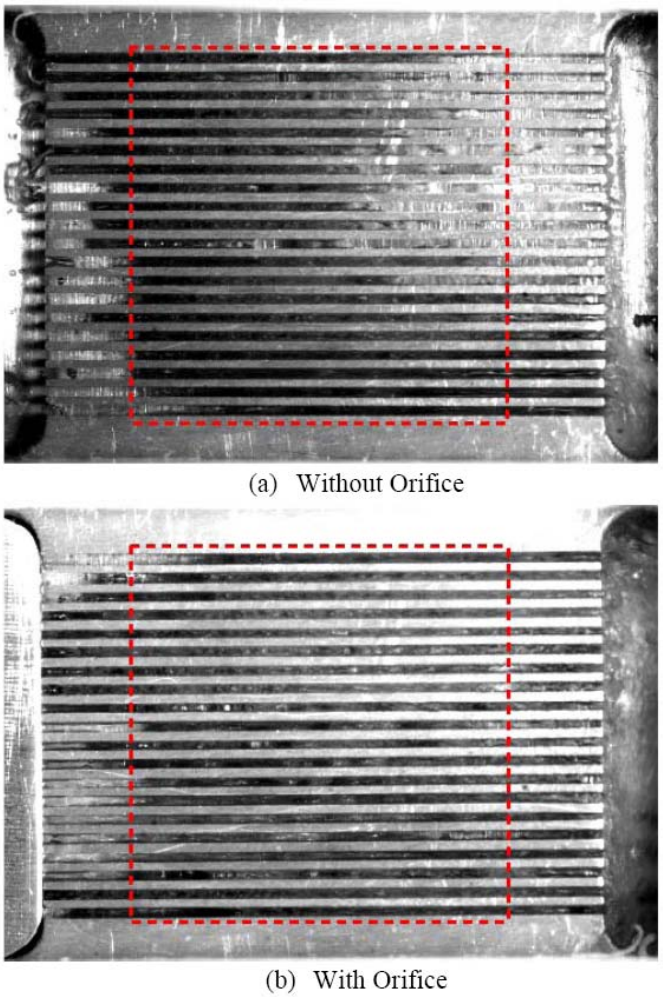

Figure 14: Flow boiling in a copper multi-microchannel test section from Park [20] showing the difference in bubble distribution a) without an inlet orifice and b) with an inlet orifice.

Figure 13 shows a sequence of video images to demonstrate back flow and parallel channel instability in a multi-microchannel element. A slug bubble was observed at the inlet of the topmost channel in (a). If the flow in the channel is pushed upstream by bubble growth downstream, the bubble goes back into the inlet plenum in (b), as there is no restriction at the channel inlet of the channel to prevent this. This reversed bubble quickly moves to one of the adjacent channels, (c), and breaks down into smaller parts before entering these channels, (d). Depending on its location, the inserted bubble becomes stagnant, (e) and (f), before moving forwards or backwards again.

Using an inlet orifice at the mouth of each microchannel can prevent backflow, instabilities and maldistribution. This may also cause the fluid to flash on entering the channels and the restriction prevents any bubbles from re-entering the inlet manifold. The results of making use of such an orifice are seen in Figure 14, clearly showing the maldistribution at the top right corner in Figure 14a without inlet orifices but excellent distribution in Figure 14b with inlet orifices. Generally, the CHF measured with orifices is much higher than that measured without [20].

C. Split flow

As far as the geometric effect is concerned, for most studies, CHF increased when the channel diameter increased and the channel length decreased under the same mass velocity and inlet temperature, as described by Wojtan *et al.* [15].

Besides the thermal goal of achieving a high CHF for a micro-evaporator cooling, the energetic goal is to operate with as low pumping power consumption as possible, and hence minimizing the two-phase pressure drop and fluid flow rate through the element are also of primary importance.

A method developed to minimise the heated length while having the same heat transfer footprint is to have the flow enter at the mid-section of the channels and split in two. Therefore, the evaporator would have one inlet and two outlets. The advantages of this setup are that heat transfer lengths are shorter, implying lower outlet vapour qualities, higher heat transfer rates and lower pressure drops. This also has the advantage that significantly higher critical heat fluxes are obtainable compared to conventional setups with one inlet and one outlet. Extensive experimental work was performed on such setups by Agostini *et al.* [21-23].

VI. Conclusion

Over the past decade, research into microchannel cooling has gained considerable attention. This is primarily due to the electronics industry requiring the removal of heat in excess of what can be achieved by conventional air-cooled methods. This paper presented some aspects of microchannel cooling, especially for two-phase cooling. Mechanisms of heat transfer were presented showing the main difference between macro and microscale boiling. The state-of-the-art heat transfer and pressure drop models were presented for simulation purposes. Simulations were run using these models to illustrate the main differences between single-phase and two-phase flows. It was shown that two-phase flow had a significant advantage over single-phase flow, having much lower temperature gradients as well as lower pressure drops, especially when channels become very small. Different radiation hard fluids were also compared, showing that CO_2 and C_2F_6 are the best for low temperature applications (<-10˚C). Of these two, CO_2 outperformed C_2F_6 due to its higher latent heat of vaporisation. This had the effect of producing much more uniform temperatures along the channel lengths.

Best practise design suggestions were given. Prediction methods were given to determine the critical heat flux of microchannel evaporators. Flow instabilities were also discussed, showing that making use of an inlet orifice at the mouth of each microchannel can prevent these instabilities as well as backflow and maldistribution. Further, by taking advantage of a split flow set-up, even higher heat transfer rates, lower pressure drops, and greater critical heat fluxes can be achieved.

VII. Nomenclature

d_i	Internal diameter	m
e	Base thickness	m
f	Frequency	Hz
G	Mass flux	kg/m^{2}s
g	Gravitational acceleration	m/s^2
H	Fin height	m
L	Channel length	m
L_{dry}	Length of vapour slug	m
L_{film}	Length of liquid film trapped by bubble	m
L_G	Length of bubble including vapour slug	m
L_L	Length of liquid slug	m
L_p	Total length of the pair of triplets	m
P	Pressure	kPa
P_{in}	Inlet pressure	kPa
P_x	Local pressure	kPa
q_b	Base heat flux	W/cm^2
R	Radius of tube	m
T	Temperature	˚C
T_b	Base temperature	˚C
T_w	Wall temperature	˚C
t	Fin thickness	m
t	Time	s
u_G	Vapour velocity	m/s
u_L	Liquid velocity	m/s
W	Channel width	m

Greek Letters

δ	Liquid film thickness	m
δ_{min}	Minimum liquid film thickness	m
δ_o	Initial liquid film thickness	m
ρ_G	Vapour density	kg/m^3
ρ_L	Liquid density	kg/m^3
σ	Surface tension	N/m
τ	Pair period	s

VIII. References

[1] B. Agostini, M. Fabbri, J. E. Park, L. Wojtan, J. R. Thome, and B. Michel, "State-of-the-art of High Heat Flux Cooling Technologies," *Heat Transfer Engineering*, vol. 28, pp. 258-281, 2007.

[2] B. Agostini, and J. R. Thome, *Comparison of an Extented Database for Flow Boiling Heat Transfer Coefficients in Multi-Microchannels Elements with the Three-Zone Model*, Castelvecchio Pascoli, Italy, 2005.

[3] A. M. Jacobi and J. R. Thome, "Heat transfer model for evaporation of elongated bubble flows in microchannels," *Journal of Heat Transfer-Transactions of the Asme*, vol. 124, pp. 1131-1136, 2002.

[4] J. R. Thome, V. Dupont, and A. M. Jacobi, "Heat transfer model for evaporation in microchannels. Part I: presentation of the model," *International Journal of Heat and Mass Transfer*, vol. 47, pp. 3375-3385, 2004.

[5] G. Ribatski, L. Wojtan, and J. R. Thome, "An analysis of experimental data and prediction methods for two-phase frictional pressure drop and flow boiling heat transfer in micro-scale channels " *Experimental Thermal and Fluid Science*, vol. 31, pp. 1-19, 2006.

[6] L. X. Cheng, G. Ribatski, J. M. Quiben, and J. R. Thome, "New prediction methods for CO2 evaporation inside tubes: Part I - A two-phase flow pattern map and a flow pattern based phenomenological model for two-phase flow frictional pressure drops," *International Journal of Heat and Mass Transfer*, vol. 51, pp. 111-124, 2008.

[7] L. X. Cheng, G. Ribatski, and J. R. Thome, "New prediction methods for CO2 evaporation inside tubes: Part II - An updated general flow boiling heat transfer model based on flow patterns," *International Journal of Heat and Mass Transfer*, vol. 51, pp. 125-135, 2008.

[8] L. X. Cheng, G. Ribatski, and J. R. Thome, "Analysis of supercritical CO2 cooling in macro- and micro-channels," *International Journal of Refrigeration-Revue Internationale Du Froid*, vol. 31, pp. 1301-1316, 2008.

[9] L. X. Cheng, G. Ribatski, L. Wojtan, and J. R. Thome, "New flow boiling heat transfer model and flow pattern map for carbon dioxide evaporating inside horizontal tubes," *International Journal of Heat and Mass Transfer*, vol. 49, pp. 4082-4094, 2006.

[10] M. H. Kim, J. Pettersen, and C. W. Bullard, "Fundamental process and system design issues in CO2 vapor compression systems," *Progress in Energy and Combustion Science*, vol. 30, pp. 119-174, 2004.

[11] J. R. Thome and G. Ribatski, "State-of-the-art of two-phase flow and flow boiling heat transfer and pressure drop of CO2 in macro- and micro-channels," *International Journal of Refrigeration-Revue Internationale Du Froid*, vol. 28, pp. 1149-1168, 2005.

[12] R. K. Shah and A. L. London, *Laminar Flow Forced Convection in Ducts*, Academic Press, New York, 1978.

[13] J. E. Park, *Critical Heat Flux in Multi-Microchannel Copper Elements with Low Pressure Refrigerants*, Swiss Federal Institute of Technology, Lausanne, 2008.

[14] R. Revellin and J. R. Thome, "An analytical model for the prediction of the critical heat flux in heated microchannels," *Int. J. Heat Mass Transfer*, vol. 51, pp. 1216-1225, 2008.

[15] L. Wojtan, R. Revellin, and J. R. Thome, "Investigation of saturated critical heat flux in a single uniformly heated microchannel," *Experimental Thermal and Fluid Science*, vol. 30, pp. 765-774, 2006.

[16] G. M. Lazarek and S. H. Black, "Evaporating Heat Transfer, Pressure Drop and Critical Heat Flux in a Small Vertical Tube with R-113," *International Journal of Heat and Mass Transfer*, vol. 25, pp. 945-960, 1982.

[17] M. B. Bowers and I. Mudawar, "High flux boiling in low flow rate, low pressure drop mini-channel and micro-channel heat sinks," *Int. J. Heat Mass Transfer*, vol. 37, pp. 321-332, 1994.

[18] W. Qu and I. Mudawar, "Measurement and correlation of critical heat flux in two-phase micro-channel heat sink," *Int. J. Heat Mass Transfer*, vol. 47, pp. 2045-2059, 2004.

[19] B. Agostini, R. Revellin, J. R. Thome, M. Fabbri, B. Michel, D. Calmi, and U. Kloter, "High Heat Flux Flow Boiling in Silicon Multi-Microchannels: Part III. Saturated Critical Heat Flux of R236fa and Two-Phase Pressure Drops," *Int. J. Heat Mass Transfer*, vol. 51, pp. 5426-5442, 2008.

[20] J. E. Park, J. R. Thome, and B. Michel, "Effect of Inlet Orifice on Saturated CHF and Flow Visualization in Multi-microchannel Heat Sinks," *Twenty-Fifth Annual Ieee Semiconductor Thermal Measurement and Management Symposium*, vol., pp. 1-8, 2009.

[21] B. Agostini, J. R. Thome, M. Fabbri, B. Michel, D. Calmi, and U. Kloter, "High heat flux flow boiling in silicon multi-microchannels - Part I: Heat transfer characteristics of refrigerant R236fa," *International Journal of Heat and Mass Transfer*, vol. 51, pp. 5400-5414, 2008.

[22] B. Agostini, J. R. Thome, M. Fabbri, B. Michel, D. Calmi, and U. Kloter, "High heat flux flow boiling in silicon multi-microchannels - Part II: Heat transfer characteristics of refrigerant R245fa," *International Journal of Heat and Mass Transfer*, vol. 51, pp. 5415-5425, 2008.

[23] B. Agostini, J. R. Thome, M. Fabbri, and B. Michel, "High heat flux two-phase cooling in silicon multimicrochannels," *IEEE Transactions on Components and Packaging Technologies*, vol. 31, pp. 691-701, 2008.